

Evidence for a backward peak in the $\gamma d \rightarrow \pi^0 d$ cross section near the η threshold

Y. Ilieva^{1,a,b}, B.L. Berman¹, A.E. Kudryavtsev^{2,1}, I.I. Strakovsky¹, V.E. Tarasov², M. Amarian²⁸, P. Ambrozewicz¹⁴, M. Anghinolfi¹⁹, G. Asryan³⁹, H. Avakian³³, H. Bagdasaryan²⁸, N. Baillie³⁸, J.P. Ball⁴, N.A. Baltzell³², V. Batourine²², M. Battaglieri¹⁹, I. Bedlinskiy², M. Bellis⁷, N. Benmouna¹, A.S. Biselli¹³, S. Bouchigny²⁰, S. Boiarinov³³, R. Bradford⁷, D. Branford¹², W.J. Briscoe¹, W.K. Brooks³³, S. Bültmann²⁸, V.D. Burkert³³, C. Butuceanu³⁸, J.R. Calarco²⁵, S.L. Careccia²⁸, D.S. Carman³³, S. Chen¹⁵, P.L. Cole¹⁷, P. Collins⁴, P. Coltharp¹⁵, D. Crabb³⁷, V. Crede¹⁵, R. De Masi⁹, E. De Sanctis¹⁸, R. De Vita¹⁹, P.V. Degtyarenko³³, A. Deur³³, R. Dickson⁷, C. Djalali³², G.E. Dodge²⁸, J. Donnelly¹⁶, D. Doughty^{10,33}, M. Dugger⁴, O.P. Dzyubak³², H. Egiyan^{33,c}, K.S. Egiyan^{39,†}, L. Elouadrhiri³³, P. Eugenio¹⁵, G. Fedotov²⁴, G. Feldman¹, H. Funsten³⁸, M. Garçon⁹, G. Gavalian^{28,d}, G.P. Gilfoyle³¹, K.L. Giovanetti²¹, F.X. Girod⁹, J.T. Goetz⁵, A. Gonenc¹⁴, R.W. Gothe³², K.A. Griffioen³⁸, M. Guidal²⁰, N. Guler²⁸, L. Guo³³, V. Gyurjyan³³, K. Hafidi³, R.S. Hakobyan⁸, F.W. Hersman²⁵, K. Hicks²⁷, I. Hleiqawi²⁷, M. Holtrop²⁵, C.E. Hyde-Wright²⁸, D.G. Ireland¹⁶, B.S. Ishkhanov²⁴, E.L. Isupov²⁴, M.M. Ito³³, D. Jenkins³⁶, H.S. Jo²⁰, K. Joo¹¹, H.G. Juengst²⁸, N. Kalantarians²⁸, J.D. Kellie¹⁶, M. Khandaker²⁶, W. Kim²², A. Klein²⁸, F.J. Klein⁸, M. Kossov², Z. Krahn⁷, L.H. Kramer^{14,33}, V. Kubarovskiy^{29,e}, J. Kuhn⁷, S.E. Kuhn²⁸, S.V. Kuleshov², J. Lachniet²⁸, J.M. Laget³³, J. Langheinrich³², D. Lawrence²³, K. Livingston¹⁶, H. Lu³², M. MacCormick²⁰, N. Markov¹¹, B. McKinnon¹⁶, B.A. Mecking³³, M.D. Mestayer³³, C.A. Meyer⁷, T. Mibe²⁷, K. Mikhailov², M. Mirazita¹⁸, R. Miskimen²³, V. Mokeev²⁴, K. Moriya⁷, S.A. Morrow^{9,20}, M. Moteabbed¹⁴, E. Munevar¹, G.S. Mutchler³⁰, P. Nadel-Turonski¹, R. Nasseripour³², S. Niccolai²⁰, G. Niculescu²¹, I. Niculescu²¹, B.B. Niczyporuk³³, M.R. Niroula²⁸, R.A. Niyazov³³, M. Nozar^{33,f}, M. Osipenko^{19,24}, A.I. Ostrovidov¹⁵, K. Park^{22,g}, E. Pasyuk⁴, C. Paterson¹⁶, J. Pierce³⁷, N. Pivnyuk², O. Pogorelko², S. Pozdniakov², J.W. Price^{6,h}, Y. Prok^{37,i}, D. Protopopescu¹⁶, B.A. Raue^{14,33}, G. Ricco¹⁹, M. Ripani¹⁹, B.G. Ritchie⁴, F. Ronchetti¹⁸, G. Rosner¹⁶, P. Rossi¹⁸, F. Sabatie⁹, C. Salgado²⁶, J.P. Santoro^{36,33,j}, V. Sapunenko³³, R.A. Schumacher⁷, V.S. Serov², Y.G. Sharabian³³, N.V. Shvedunov²⁴, E.S. Smith³³, L.C. Smith³⁷, D.I. Sober⁸, A. Stavinsky², S.S. Stepanyan²², S. Stepanyan³³, B.E. Stokes¹⁵, P. Stoler¹⁹, S. Strauch³², M. Taiuti¹⁹, D.J. Tedeschi³², U. Thoma^{33,k}, A. Tkabladze¹, S. Tkachenko²⁸, C. Tur³², M. Ungaro¹¹, M.F. Vineyard³⁵, A.V. Vlassov², D.P. Watts¹², L.B. Weinstein²⁸, D.P. Weygand³³, M. Williams⁷, E. Wolin³³, M.H. Wood^{32,1}, A. Yegneswaran³³, L. Zana²⁵, J. Zhang²⁸, B. Zhao¹¹, and Z. Zhao³²
(The CLAS collaboration)

¹The George Washington University, Washington, District of Columbia 20052

²Institute of Theoretical and Experimental Physics, Moscow, 117259, Russia

³Argonne National Laboratory, Argonne, Illinois 60439

⁴Arizona State University, Tempe, Arizona 85287

⁵University of California at Los Angeles, Los Angeles, California 90095

⁶California State University, Dominguez Hills, Carson, California 90747

⁷Carnegie Mellon University, Pittsburgh, Pennsylvania 15213

⁸Catholic University of America, Washington, District of Columbia 20064

⁹CEA-Saclay, Service de Physique Nucléaire, F91191 Gif-sur-Yvette, France

^a On leave from: INRNE, BAS, Sofia, Bulgaria

^b Current address: USC, Columbia, South Carolina 29208

^c Current address: UNH, Durham, NH 03824

^d Current address: UNH, Durham, NH 03824

^e Current address: Jefferson Lab, Newport News, VA 23606

^f Current address: TRIUMF, Vancouver, Canada V6T 2A3

^g Current address: Jefferson Lab, Newport News, VA 23606

^h Current address: UCLA, Los Angeles, CA 90095

ⁱ Current address: MIT, Cambridge, MA 02139

^j Current address: CUA, Washington, DC 20064

^k Current address: HISKP, University of Bonn, 53115 Bonn, Germany

¹ Current address: UMass, Amherst, MA 01003

- ¹⁰Christopher Newport University, Newport News, Virginia 23606
¹¹University of Connecticut, Storrs, Connecticut 06269
¹²Edinburgh University, Edinburgh EH9 3JZ, United Kingdom
¹³Fairfield University, Fairfield, Connecticut 06824
¹⁴Florida International University, Miami, Florida 33199
¹⁵Florida State University, Tallahassee, Florida 32306
¹⁶University of Glasgow, Glasgow G12 8QQ, United Kingdom
¹⁷Idaho State University, Pocatello, Idaho 83209
¹⁸INFN, Laboratori Nazionali di Frascati, 00044 Frascati, Italy
¹⁹INFN, Sezione di Genova, 16146 Genova, Italy
²⁰Institut de Physique Nucleaire ORSAY, Orsay, France
²¹James Madison University, Harrisonburg, Virginia 22807
²²Kyungpook National University, Daegu 702-701, Republic of Korea
²³University of Massachusetts, Amherst, Massachusetts 01003
²⁴Moscow State University, General Nuclear Physics Institute, 119899 Moscow, Russia
²⁵University of New Hampshire, Durham, New Hampshire 03824
²⁶Norfolk State University, Norfolk, Virginia 23504
²⁷Ohio University, Athens, Ohio 45701
²⁸Old Dominion University, Norfolk, Virginia 23529
²⁹Rensselaer Polytechnic Institute, Troy, New York 12180
³⁰Rice University, Houston, Texas 77005
³¹University of Richmond, Richmond, Virginia 23173
³²University of South Carolina, Columbia, South Carolina 29208
³³Thomas Jefferson National Accelerator Facility, Newport News, Virginia 23606
³⁴TRIUMF, Vancouver, Canada V6T 2A3
³⁵Union College, Schenectady, NY 12308
³⁶Virginia Polytechnic Institute and State University, Blacksburg, Virginia 24061
³⁷University of Virginia, Charlottesville, Virginia 22901
³⁸College of William and Mary, Williamsburg, Virginia 23187
³⁹Yerevan Physics Institute, 375036 Yerevan, Armenia
† deceased

Received: date / Revised version: date

Abstract High-quality cross sections for the reaction $\gamma d \rightarrow \pi^0 d$ have been measured using the CLAS at Jefferson Lab over a wide energy range near and above the η -meson photoproduction threshold. At backward c.m. angles for the outgoing pions, we observe a resonance-like structure near $E_\gamma=700$ MeV. Our model analysis shows that it can be explained by η excitation in the intermediate state. The effect is the result of the contribution of the $N(1535)S_{11}$ resonance to the amplitudes of the subprocesses occurring between the two nucleons and of a two-step process in which the excitation of an intermediate η meson dominates.

PACS. 13.60.Le Meson Production – 14.20.Gk Baryon resonances with $S = 0$ – 25.20.Lj Photoproduction reactions

1 Introduction

Interactions of the η meson with few-nucleon systems complement our knowledge of the η -nucleon interaction. Interest in these systems stems from the hypothetical existence of η -nuclear quasibound states. Such states have been predicted by Haider and Liu [1] and Li, Cheung, and Kuo [2]. Although there has been no direct experimental verification of this hypothesis to date, there is mounting evidence that such states might exist in the lightest few-nucleon systems [3–5].

For the case of the three-nucleon system, it was found at Saclay that the $dp \rightarrow \eta^3\text{He}$ production amplitude falls rapidly just above the η threshold [3]. A less pronounced slope was found in the $dd \rightarrow \eta^4\text{He}$ amplitude [4]. For the two-nucleon system, very strong final-state interactions

(FSI) were found in the $pp \rightarrow pp\eta$ cross section in the threshold region [5]. The energy dependence of the $NN \rightarrow NN\eta$ and $NN \rightarrow d\eta$ reactions can be understood in terms of NN FSI ([6] and references therein). However, as noted in Ref. [7], the existence of a narrow virtual state in the η -deuteron system can be inferred.

The production of a virtual η meson may also play a role in other nuclear reactions, even in those for which there is no η in either the initial or the final state, but only in an intermediate state. Examples are the reactions $pd \rightarrow \pi^+ {}^3\text{H}$ and $pd \rightarrow \pi^0 {}^3\text{He}$, for which there are strong indications that an intermediate η cusp is present [8]. Evidence for an intermediate η meson also was found in elastic πd backward scattering. This contribution manifests itself as a cusp in the energy dependence of the backward

differential cross sections near the η threshold. The effect was predicted in Ref. [9] and was confirmed by several independent measurements of backward πd scattering [10]. In this work, we present the first systematic evidence for a similar phenomenon (the first indication was found in Ref. [11]) in the coherent photoproduction of a neutral pion on the deuteron, $\gamma d \rightarrow \pi^0 d$.

All of the above phenomena take place because η -meson production in hadron-hadron collisions near threshold is enhanced. This is because the cross section for excitation of the nearby baryonic resonance $N(1535)S_{11}$ is large and this resonance is strongly coupled to the ηN channel. Since the amplitudes for photoproduction of the $N(1535)S_{11}$ are also large [12–14], one can expect a similar enhancement in various photonuclear reactions.

Recently, coherent photoproduction of the π^0 meson from the deuteron was studied theoretically [15]. In particular, it was demonstrated that at large c.m. scattering angles and photon energies E_γ between 600 and 800 MeV, the two-step process with the excitation of an intermediate η -meson (shown in Fig. 1(b)) dominates over single-step photoproduction (shown in Fig. 1(a)) and pion rescattering. This two-step process can be analyzed as two sequential subprocesses: $\gamma N_1 \rightarrow N(1535) \rightarrow \eta N_1$ and $\eta N_2 \rightarrow N(1535) \rightarrow \pi^0 N_2$, where N_1 and N_2 are the two nucleons in the deuteron. It was shown in [15] that this mechanism explains qualitatively the structure in the $\gamma d \rightarrow \pi^0 d$ differential cross section, which we present here, at large angles and for $E_\gamma \sim 600$ –800 MeV. The main conclusions of Ref. [15] were reproduced in a more recent paper [16], where it was shown that in addition to this two-step process, the full dynamics in the intermediate $NN\eta$ system could be important as well. Other theoret-

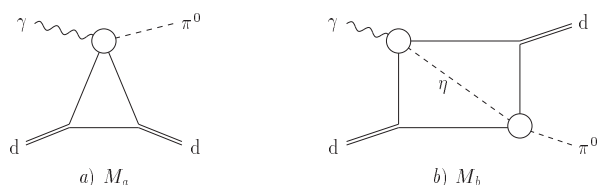


Fig. 1. Feynman diagrams for the $\gamma d \rightarrow \pi^0 d$ reaction considered in [15]: (a) single-scattering amplitude M_a ; (b) double-scattering amplitude M_b . It was shown in [15] that (b) dominates over (a) at backward angles for $E_\gamma \sim 700$ MeV.

ical studies of the $\gamma d \rightarrow \pi^0 d$ reaction can be found in a number of papers [17]. However, none of these considers the effect of the opening of the η threshold at 700 MeV.

Our photoproduction data, presented here, give for the first time clear evidence for a prominent effect around 700 MeV at large c.m. angles, which can be explained by the excitation of an intermediate η meson.

2 Experiment

The experiment took place in Hall B at Jefferson Lab using the CEBAF Large Acceptance Spectrometer (CLAS) [18].

A collimated, tagged, real-photon beam, with energies between 0.5 and 2.3 GeV was incident on a 10-cm-long LD₂ target installed in the center of the CLAS. The energies of the photons were tagged using the Hall-B tagger [19]. The outgoing deuterons were tracked in the six toroidal magnetic spectrometers of the CLAS. They were bent outwards by the magnetic field, and their trajectories were measured by three layers of drift chambers surrounding the LD₂ target. The time of flight of the deuterons was measured by 6×48 scintillators (TOF) that surround the CLAS detector outside of the magnetic field. A set of six scintillator counters, comprising the start counter and placed just around the target, measured the event time at the vertex. The CLAS covers the polar angular range between 8° and 142° in the laboratory system and the entire range in azimuthal angle.

3 Data Analysis

Since the CLAS has very good acceptance for charged particles, and a very limited one for neutrals, the analysis of the $\gamma d \rightarrow \pi^0 d$ reaction was based on detecting the final-state deuterons and selecting the good events by the missing-mass technique. Deuterons were identified from their time of flight and momentum, which allowed a mass reconstruction. Thus, the initial event selection was done based on the reconstructed mass. Further selection of events was achieved by comparing the event vertex time with the photon vertex time as measured by the tagger. Low-momentum protons were discarded based on a cut on the particle momentum *vs.* energy loss in the TOF. In addition, fiducial cuts were applied to the remaining data sample in order to remove edge areas of the detector where the acceptance was not well reproduced by a simulation.

Once the data were reduced, based on all of the above cuts, they were binned in photon energy and pion c.m. scattering angle ($E_\gamma, \cos\theta_\pi^*$). Here, we present differential cross sections for the reaction $\gamma d \rightarrow \pi^0 d$ based on a photon-energy bin width of 25 MeV and a $\cos\theta_\pi^*$ bin width of 0.1. For every such ($E_\gamma, \cos\theta_\pi^*$) bin, we determined the reaction yields after sideband background subtraction was performed on the missing-mass (mm_d^2) distributions as shown in Fig. 2. The quantity mm_d^2 is defined as $mm_d^2 = (p_\gamma + p_t - p_d)^2$, where p_γ , p_t , and p_d are the four-momentum vectors of the beam, the target, and the recoil deuteron, respectively. The systematic uncertainty associated with the background subtraction depends on the kinematic bin, and varies between 1.5% and 6.4%. The statistical uncertainty of the extracted yields is also bin-dependent, and varies between 3% and 30%.

4 Results

Differential cross sections were obtained by normalizing the true-event yields to the photon flux, the number of target scattering centers, and the CLAS acceptance [20]. The statistical uncertainty of the photon flux is negligible.

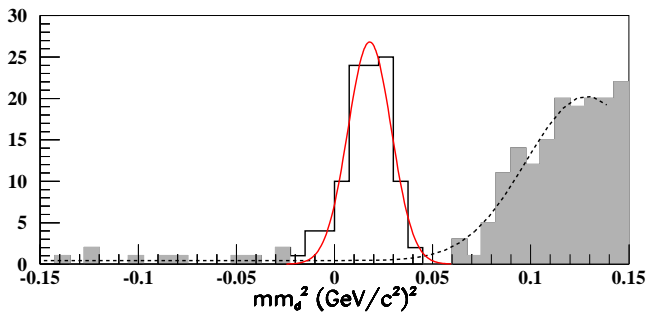


Fig. 2. An example of the background subtraction, for the bin $0.675 < E_\gamma < 0.7$ GeV and $-0.8 < \cos\theta_\pi^* < -0.7$. One sees that the pion peak is well separated from the background. The contribution of the latter to the peak is $< 10\%$. The shaded areas show the sidebands around the pion peak we used in order to determine the shape and the magnitude of the background underneath it.

The systematic uncertainty of the evaluated photon flux is 3.3%. The statistical uncertainty associated with the calculated CLAS acceptance is bin-dependent and varies between 0.8% and 2.5%. The systematic uncertainty of the acceptance is less than 10%. A common factor of $1.0141 \pm 0.0006^{stat} \pm 0.0005^{syst}$, due to the inefficiency of the procedure for choosing the right photon for a given event, was applied to all of the differential cross sections. There is also an overall systematic uncertainty of 0.5% related to the determination of the target length and density [21]. Thus, the total uncertainty of the differential cross sections is bin-dependent and varies smoothly from 11% to 33%.

Our differential cross sections for the reaction $\gamma d \rightarrow \pi^0 d$ for five c.m. angular bins are shown in Fig. 3. Note that some of the angular bins overlap partially with each other. The latter is due to the fact that for a consistency check, we determined differential cross sections for two entirely separate angular binnings. The figure illustrates the consistency of the structure and the model interpretation at different kinematical binnings.

Overall, our data are in very good agreement with previously measured differential cross sections [11, 22–24]. However, in the range of photon energies where we observe the backward peak discussed here, the data of Ref. [11] exhibit a structure but of a smaller magnitude, whereas the data of Ref. [23] do not exhibit any structure. In order to understand this discrepancy we performed many consistency checks, and our analysis procedure was studied in great detail for possible sources of errors [20]. The structure near 0.7 GeV and its magnitude persists. Both of the measurements [11, 23] were done at the same accelerator facility and used an untagged bremsstrahlung beam, which might introduce large systematic uncertainties in the determination of the photon flux.

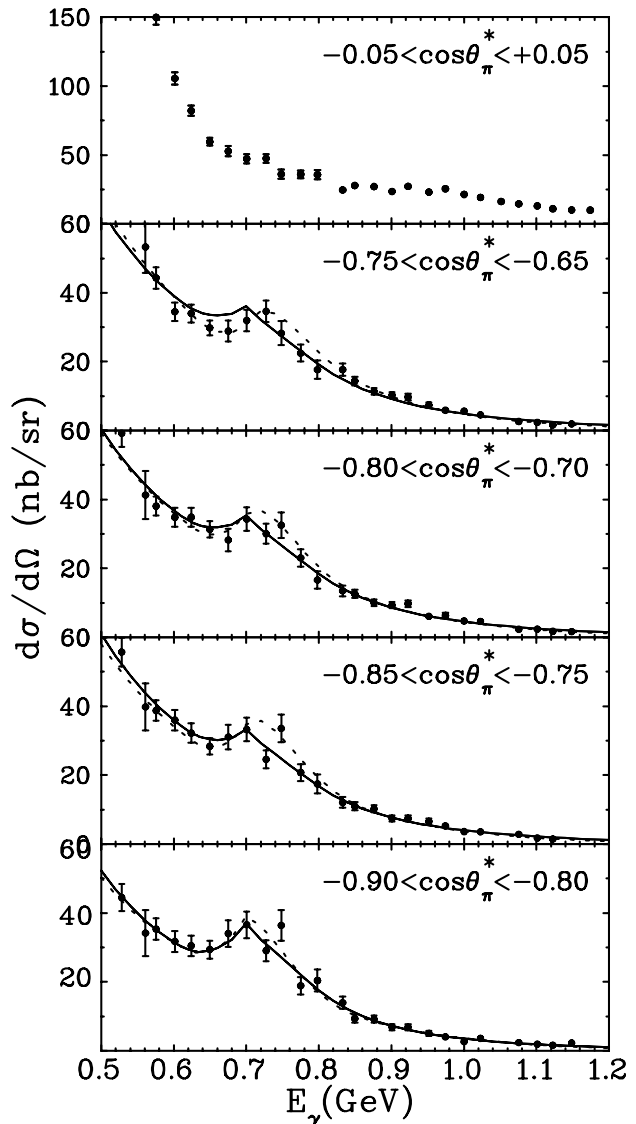


Fig. 3. Excitation functions for the reaction $\gamma d \rightarrow \pi^0 d$ for several bins in $\cos\theta_\pi^*$. The filled circles are our CLAS data. The error bars show the total bin-dependent uncertainty for each data point. The dashed and solid curves are the results of fit 1 and fit 2 (see the text), respectively, obtained with the helicity amplitudes from Ref. [13] (set (2)). One sees that the excitation function at $\cos\theta_\pi^* = 0.0$ does not exhibit any prominent structure near 0.7 GeV. Note that some of the angular bins overlap partially with each other.

5 Discussion

To achieve a quantitative understanding of our data, we employ the semiphenomenological description of Ref. [15]. We express the reaction amplitude M as a sum $M = M_1 S + M_2 S$, where $M_1 S$ is the two-step amplitude M_b given by the diagram in Fig. 1(b) and calculated in Ref. [15] with intermediate η production, and S is a spin factor. $M_2 S$ is the effective “background” amplitude which takes into account all possible background diagrams (including the single-scattering amplitude M_a shown in Fig. 1(a)). We parametrize it as $M_2 = A \exp(i\varphi_2 - bE_\gamma)$, where φ_2 is

the phase. The square of the total amplitude with unpolarized particles is then written as $|M|^2 = |M_1 + M_2|^2 |S|^2$ and is applied to describe the experimental excitation functions for given values of $\cos \theta_\pi^*$. We give the results of fits for two different parametrizations of φ_2 :

$$\text{fit 1: } \varphi_2(E_\gamma) = \alpha + \beta (E_\gamma - 0.7 \text{ GeV}); \quad (1)$$

$$\text{fit 2: } \varphi_2(E_\gamma) = \alpha + \varphi_1(E_\gamma). \quad (2)$$

For fit 1, we use a linear E_γ -dependent background phase $\varphi_2(E_\gamma)$ with two parameters, α and β . We define $\alpha = \varphi_2(E_\gamma)$ at energy $E_\gamma = 0.7$ GeV, where “by eye” the amplitude M_1 peaks. Thus, we use four parameters (A , b , α , and β) in fit 1.

For fit 2, we use the parameter α as the relative phase of the amplitudes M_1 and M_2 , *i.e.*, $\alpha = \varphi_2(E_\gamma) - \varphi_1(E_\gamma)$, where $\varphi_1(E_\gamma)$ is the phase of the amplitude M_1 and is a given function. Thus, we use three parameters (A , b , and α) in fit 2. In both variants all the parameters were varied independently to fit the data for various values of $\cos \theta_\pi^*$.

We note that the two-step amplitude M_1 with intermediate η production is proportional to $A_{1/2}^p - A_{1/2}^n$, where $A_{1/2}^p$ ($A_{1/2}^n$) is the helicity amplitude of the decay $N(1535) \rightarrow p\gamma$ ($n\gamma$). Values for these amplitudes vary widely in the literature. Here, we give some sets (in units of $10^{-3} \text{ GeV}^{-1/2}$):

$$(1) A_{1/2}^p = 107, A_{1/2}^n = -96 \text{ ([14])};$$

$$(2) A_{1/2}^p = 78, A_{1/2}^n = -50 \text{ ([13], used in [15])};$$

$$(3) A_{1/2}^p = 60, A_{1/2}^n = -20 \text{ ([25])}.$$

The results for the free parameters from the data fitting are given in Table 1 for large values of θ_π^* . Here, the coupling set (2) was used. The dashed and the solid curves in Fig. 3 correspond to the results of fits 1 and 2, respectively, and both fits give a satisfactory description of the data. The corresponding values of χ^2/N (N is the number of degrees of freedom) are also given in Table 1. Using this procedure, we obtain a good description of the data at large scattering angles ($\cos \theta_\pi^* < -0.5$), where the η effect is strongly pronounced. We do not consider the data at smaller angles because a more complicated parametrization of the background is needed and in any case the effect is less pronounced.

The backward-angle structure is qualitatively reproduced using various sets of couplings $A_{1/2}^p$ and $A_{1/2}^n$. We obtained also a good description (not shown) using coupling set (1) in fit 2 and set (3) in fits 1 and 2. Thus, the experimentally observed enhancement in the excitation functions near $E_\gamma \sim 0.7$ GeV needs no exotic explanation such as was done, for instance, in Ref. [11].

In order to evaluate the statistical significance of the structure exhibited by our data, we performed a χ^2 test of goodness of fit. We tested the hypothesis that the excitation functions at large angles, which are shown in Fig. 3, can be described by a smooth function. We used the amplitude M_2 , which falls off smoothly with E_γ and describes well the experimental data outside the energy range where the enhancement is observed, to fit the excitation functions at large angles. The results for the χ^2 and the significance level of this hypothesis (the P-value) are given in

Table 2. χ^2 and number of degrees of freedom N of the fits to the large angle excitation functions with the smooth amplitude M_2 . The significance of the hypothesis (the P-value for the χ^2 test of goodness of fit) that M_2 describes the data is also shown.

$\cos \theta_\pi^*$	χ^2	N	P-value
-0.7	44.43	22	0.003
-0.75	43.68	22	0.004
-0.8	35.71	21	0.02
-0.85	77.07	22	0.0001

Table 2. We see that the probability that this hypothesis is true is smaller than 2%. Thus, the statistical significance of the structure is greater than 98%.

Finally, the excitation of the $N(1535)S_{11}$ resonance depends on the initial polarization of the beam and target. The spin factor S of the two-step amplitude with an intermediate η meson and an S -wave deuteron wave function is $S = (\boldsymbol{\epsilon}_2^* \cdot [\mathbf{e} \times \boldsymbol{\epsilon}_1])$, where \mathbf{e} and $\boldsymbol{\epsilon}_1$ ($\boldsymbol{\epsilon}_2$) are the polarization 3-vectors of the initial photon and the initial (final) deuteron. For an unpolarized final-state deuteron and for $\lambda_\gamma = \pm 1$ and $\lambda_d = 0, \pm 1$ as the helicities of the initial photon and deuteron, respectively, we obtain $|S|^2 = 2/3$ for unpolarized particles; $|S|^2 = 1$ for $\lambda_d = 0, -\lambda_\gamma$; and $|S|^2 = 0$ for $\lambda_d = \lambda_\gamma$. Thus, for $\lambda_d = 0, -\lambda_\gamma$, we expect the η -effect to be enhanced compared with the unpolarized case. For $\lambda_d = \lambda_\gamma$ (parallel polarization of the initial photon and deuteron), the excitation of the $N(1535)S_{11}$, and hence the η -effect, should be suppressed.

6 Summary

To summarize, we have measured unpolarized differential cross sections for the $\gamma d \rightarrow \pi^0 d$ reaction at backward c.m. angles and for photon energies above 500 MeV. The data show a pronounced structure (with statistical significance greater than 98%) in the excitation functions in the region of 700 MeV. For the first time, this phenomenon is systematically studied with good accuracy. The structure can be explained by the opening of the η -photoproduction threshold on a single nucleon, and in our model is mainly related to the excitation of the intermediate resonance $N(1535)S_{11}$ in a two-step process. The details of the underlying dynamics can be further explored via polarization measurements.

Acknowledgement

We would like to acknowledge the efforts of the staff of the Accelerator and the Physics Divisions at Jefferson Lab that made this experiment possible. This work was supported by the U. S. Department of Energy under grant DE-FG02-95ER40901, in part under grant DE-FG02-99ER41110, by the grant of the Russian Ministry of Industry, Science, and Technology NSh 5603.2006.2, by the Science and Technology Facilities Council (STFC), and by

Table 1. Parameters and χ^2 per degree of freedom N of the model-based fits, explained in the text, to the experimental excitation functions at large c.m. angles. Parameters A , b , α , and β (A , b , and α) were used in fit 1 (fit 2). The values for the helicity amplitudes $A_{1/2}^{p,n}$ used in the calculations were taken from Ref. [12] (set (2)). $N = N_{dat} - N_{par}$, where $N_{par} = 4(3)$ for fit 1(2). $N_{dat} = 24$ for $\cos \theta_\pi^* = -0.8$, and 25 for the others.

$\cos \theta_\pi^*$	fit	A	b (GeV $^{-1}$)	α (deg)	β (deg/MeV)	χ^2/N
-0.7	1	1.68	2.53	177	0.79	1.12
-0.7	2	1.55	2.40	59		1.73
-0.75	1	1.57	2.51	156	0.80	1.27
-0.75	2	1.52	2.42	59		1.07
-0.8	1	1.69	2.68	158	0.81	1.55
-0.8	2	1.63	2.55	66		0.83
-0.85	1	1.51	2.59	136	0.89	0.99
-0.85	2	1.55	2.61	42		0.79

the National Research Foundation of Korea. The South-eastern Universities Research Association (SURA) operated the Thomas Jefferson National Accelerator Facility for the United States Department of Energy under contract DE-AC05-84ER40150 until May 31, 2006.

References

1. Q. Haider and L. C. Liu, Phys. Lett. B 172 (1986) 257; L. C. Liu and Q. Haider, Phys. Rev. C 34 (1986) 1845.
2. G. L. Li, W. K. Cheung, and T. T. Kuo, Phys. Lett. B 195 (1987) 515.
3. B. Mayer *et al.*, Phys. Rev. C 53 (1996) 2068.
4. N. Willis *et al.*, Phys. Lett. B 406 (1997) 14.
5. A. M. Bergdolt *et al.*, Phys. Rev. D 48 (1993) R2969; E. Chiavassa *et al.*, Phys. Lett. B 322 (1994) 270; H. Calen *et al.*, Phys. Lett. B 366 (1996) 39; J. Smyrski *et al.*, Phys. Lett. B 474 (2000) 182.
6. V. Baru *et al.*, Phys. Rev. C 67 (2003) 024002.
7. S. Wycech and A. M. Green, Phys. Rev. C 64 (2001) 045206.
8. M. Abdel-Bary *et al.* [GEM Collaboration], Phys. Rev. C 68 (2003) R021603.
9. L. A. Kondratyuk and F. M. Lev, Yad. Fiz. 23 (1976) 1056 [former Sov. J. Nucl. Phys. 27 (1976) 441].
10. R. Keller *et al.*, Phys. Rev. D 11 (1975) 2389; B. M. Abramov *et al.*, Nucl. Phys. A 372 (1981) 301; M. Akemoto *et al.*, Phys. Rev. Lett. 50 (1983) 400.
11. A. Imanishi *et al.*, Phys. Rev. Lett. 54 (1985) 2497.
12. R. A. Arndt *et al.*, Phys. Rev. C 66 (2002) 055213.
13. R. A. Arndt *et al.*, Phys. Rev. C 42 (1990) 1864.
14. G. Knöchlein, D. Drechsel, and L. Tiator, Z. Phys. A 352 (1995) 327.
15. A. E. Kudryavtsev *et al.*, Phys. Rev. C 71 (2005) 035202.
16. A. Fix, Eur. Phys. J. A 26 (2005) 293.
17. T. Miyachi, H. Tezuka, and Y. Morita, Phys. Rev. C 36 (1987) 844; H. Garcilazo and E. Moya de Guerra, Phys. Rev. C 52 (1995) 49 and references therein; S. S. Kamalov, L. Tiator, and C. Bennhold, Phys. Rev. C 55 (1997) 98.
18. B. Mecking *et al.* [CLAS Collaboration], Nucl. Instrum. Methods Phys. Res. A 503 (2003) 513.
19. D. I. Sober *et al.* [CLAS Collaboration], Nucl. Instrum. Methods Phys. Res. A 440 (2000) 263.
20. Y. Ilieva, *Coherent Pion Photoproduction on Deuterium: $\gamma d \rightarrow \pi^0 d$* , CLAS-NOTE 2007-006; www1.jlab.org/ul/Physics/Hall-B/clas/index.cfm.
21. M. Mirazita *et al.* [CLAS Collaboration], Phys. Rev. C 70 (2004) 014005.
22. K. Baba *et al.*, Phys. Rev. C 28 (1983) 286.
23. M. Asai *et al.*, Phys. Lett. B 187 (1987) 249; Y. Sumi, private communication.
24. D. G. Meekins *et al.*, Phys. Rev. C 60 (1999) 052201.
25. R. A. Arndt, I. I. Strakovsky, and R. L. Workman, Phys. Rev. C 53 (1996) 430.